Control of Secondary Electron Emission Flux through Surface Geometry

Research Review Seminar
February 9, 2018

Charles Swanson

Introduction

- The phenomenon of Secondary Electron Emission (SEE)
- Modeling considerations
- Practical applications
- The phenomenon of SEE suppression by surface geometry
- Candidate geometries
- Tungsten fuzz in tokamak divertors
- Other industrial applications for these surfaces
- The tool: Monte-Carlo simulation
- Our work:
    - Velvet
    - Feathers
    - Fuzz/foam
- Conclusions
- References

The phenomenon of Secondary Electron Emission (SEE)

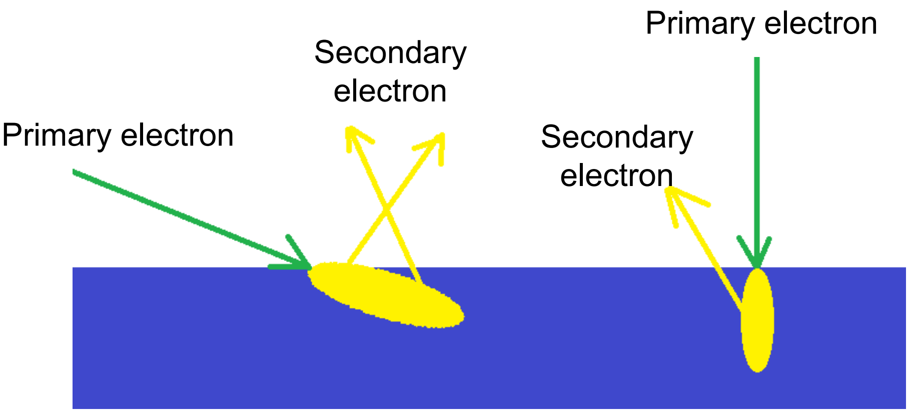

High-energy electrons collide with electrons in a surface. Some are able to escape.

Secondary electrons are emitted with flux weighted in the normal direction, $P(\Omega) = \cos\theta$
Bronstein, Vtorichnaya Elektronnaya Emissiya (1969) [3]

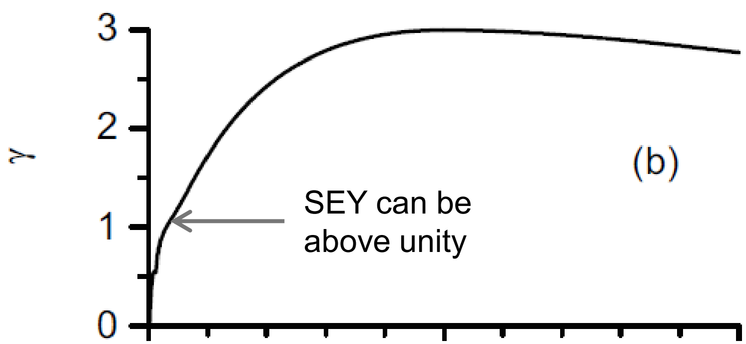

Secondary Electron Yield (SEY) follows a universal curve, usually tabulated empirically. Shown is that of Scholtz, Philips J. Res. (1996) [1]. Figure from Sydorenko, PhD thesis (2006) [2]

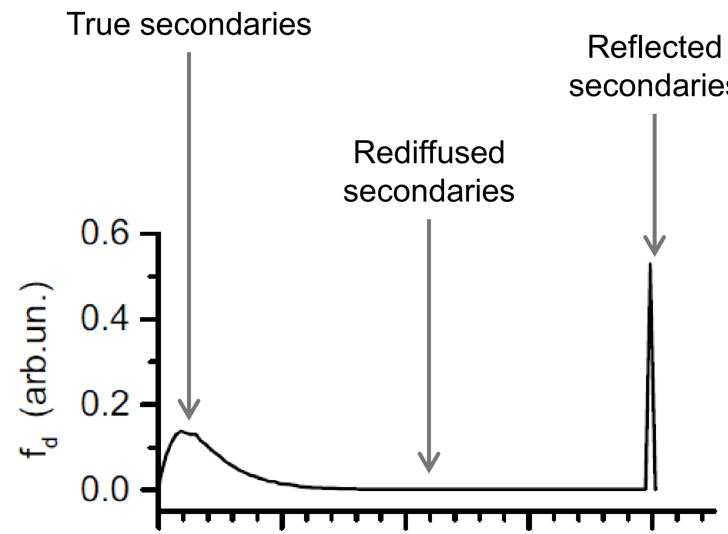

Secondary Electron flux is made of "true" secondaries (approximately Maxwellian), "rediffused" secondaries (approximately uniform in energy), and "reflected" secondaries (same energy as primary). Figure from Sydorenko, PhD thesis (2006) [2]

Modeling considerations

SEE is ubiquitous. It occurs whenever plasma touches a surface. Sheath-heated secondary electrons may alter ionization profiles, or secondaries may eliminate sheaths entirely.

Secondary electrons

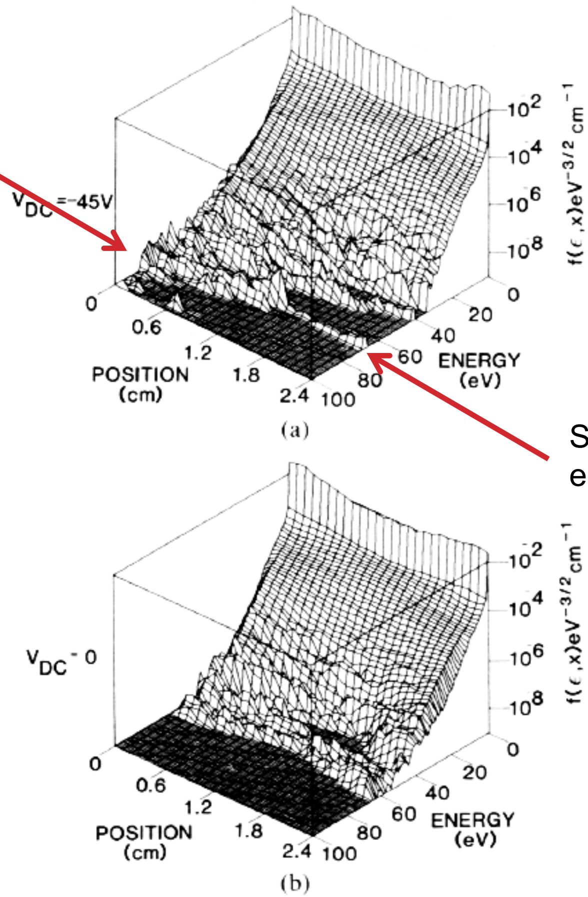

Secondary electrons

SEE from a very biased electrode can inject fast electrons which penetrate deep into your system, ruining your fluid model. Kushner, IEEE Trans. Plasma Science (1986) [5]

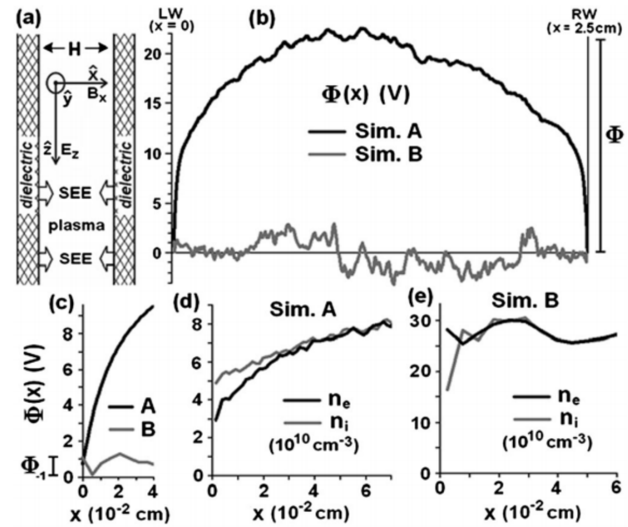

SEE can alter potential profiles. Strong SEE can make sheaths literally disappear. Sim. B is with net Secondary Electron Yield (SEY) of 1. Campanell, Phys Rev Lett (2012) [4]

Practical applications

Materials processing, RF cavities, Hall Thrusters, particle accelerators

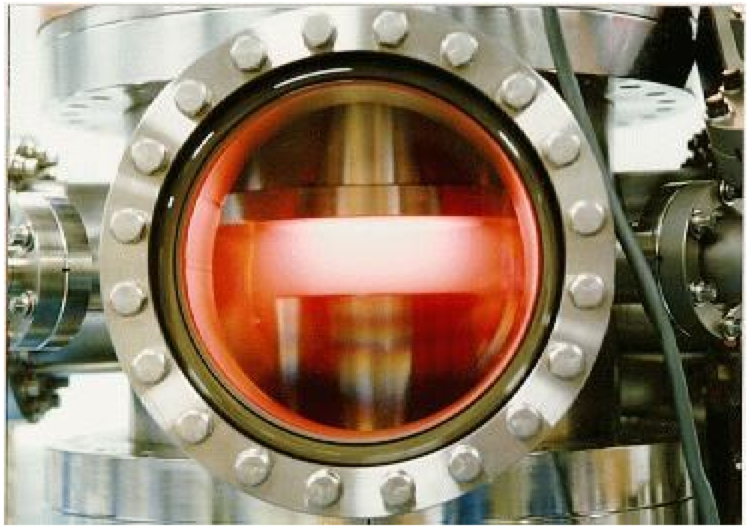

Photo from http://www.utdallas.edu/~overzet/PALpict.htm

Secondary electrons

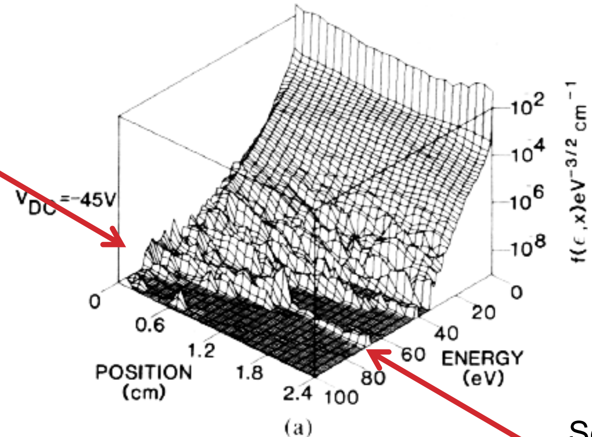

Secondary electrons

SEE from a very biased electrode injecting fast electrons which drastically alter the ionization profile in a capacitively coupled etching device. Kushner, IEEE Trans. Plasma Science (1986) [5]

Many integrated circuit operations are performed in Capacitively Coupled plasma reactors. Secondary electrons often provide the majority of ionization in such systems, and can account for the majority of power coupled to the plasma [5]

Practical applications

Materials processing, **RF cavities**, Hall Thrusters, particle accelerators

By Bukvoed - Own work, CC BY-SA 3.0,
https://commons.wikimedia.org/w/index.php?curid=4840831

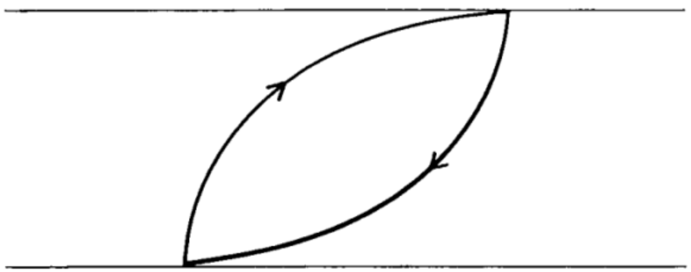

Multipactor effect limiting efficiency in an RF cavity. Figure from Vaughan, IEEE Trans. Electron Devices (1988) [6]

RF cavities and amplifiers can have their total throughput limited by the Multipactor effect, a condition of secondary electron amplification [6]

Practical applications

Materials processing, RF cavities, **Hall Thrusters**, particle accelerators

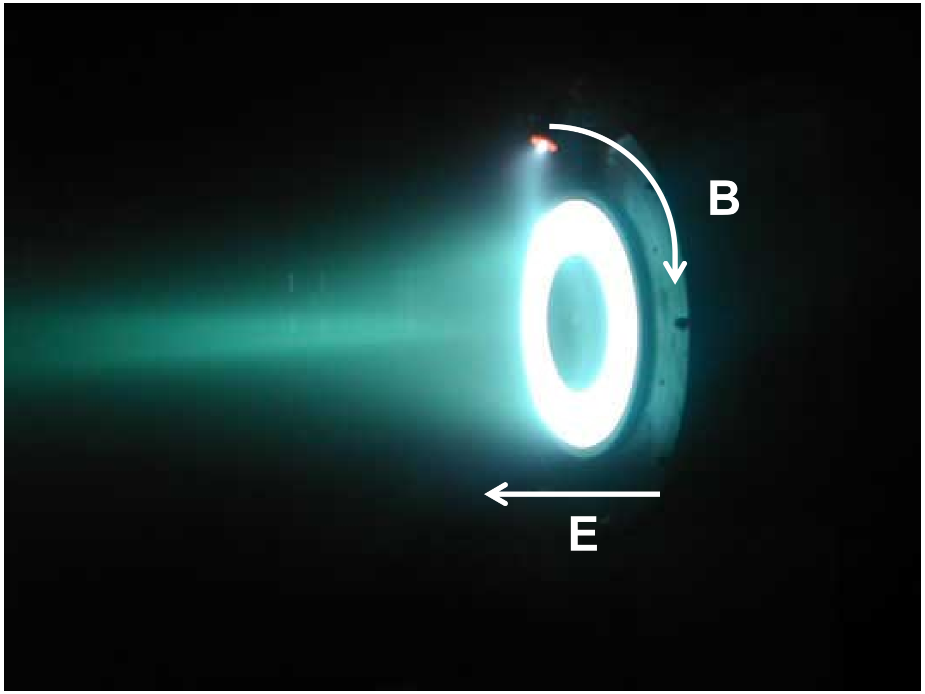

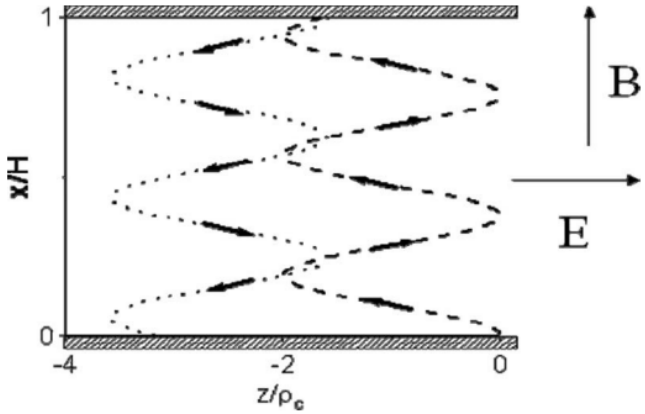

Figure from Kaganovich *et. al.,* Phys. Plasmas (2007) [7]

Photo from https://en.wikipedia.org/wiki/Hall-effect_thruster

In a Hall Thruster, Ion current produces thrust while electron current is useless. Electron current is impeded magnetically.

SEE can cause electron current in a Hall Thruster by allowing secondary electrons to migrate down the walls [7]

Practical applications

Materials processing, RF cavities, Hall Thrusters, **particle accelerators**

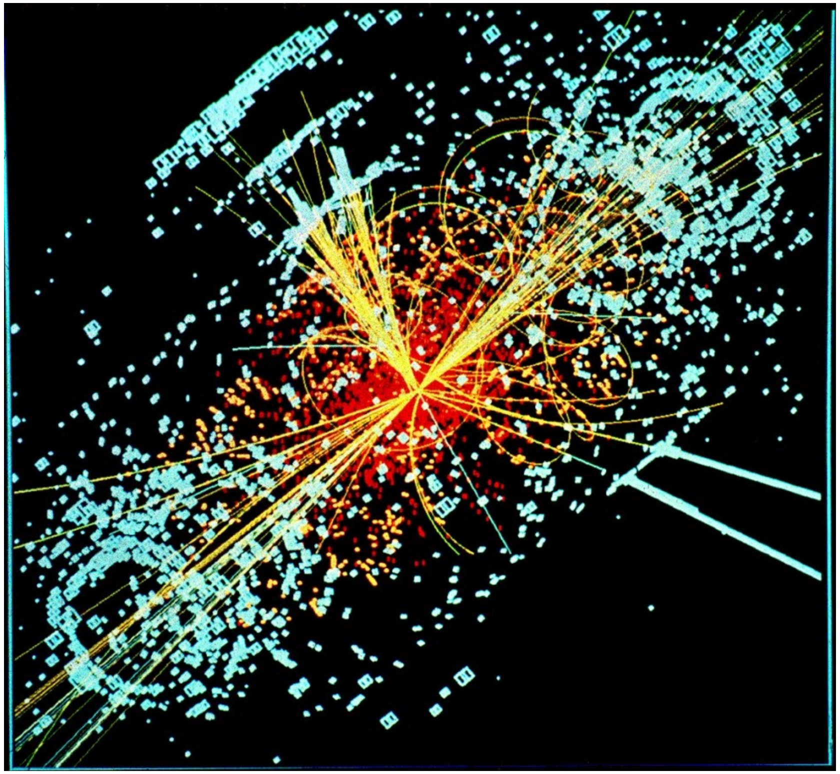

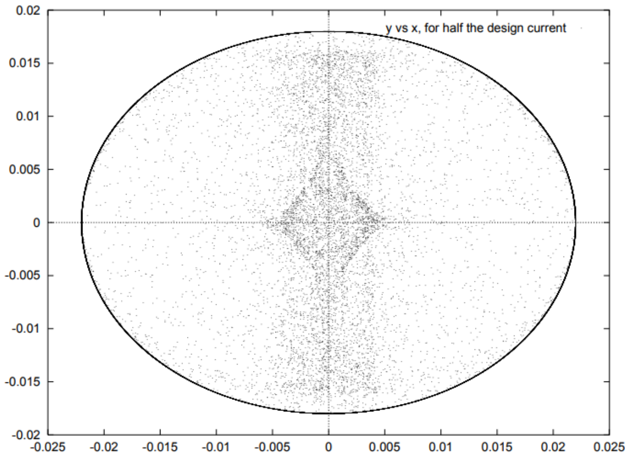

Simulation of SEE space charge in the LHC, Zimmermann, CERN-LHC-PROJECT-REPORT-95 (1997) [8]

Photo from https://en.wikipedia.org/wiki/Large_Hadron_Collider

SEE space charge is known to de-focus particle beams like the Large Hadron Collider. [8] Accelerator communities like the LHC are responsible for some of the research on SEE mitigation [9].

The phenomenon of SEE suppression by surface geometry

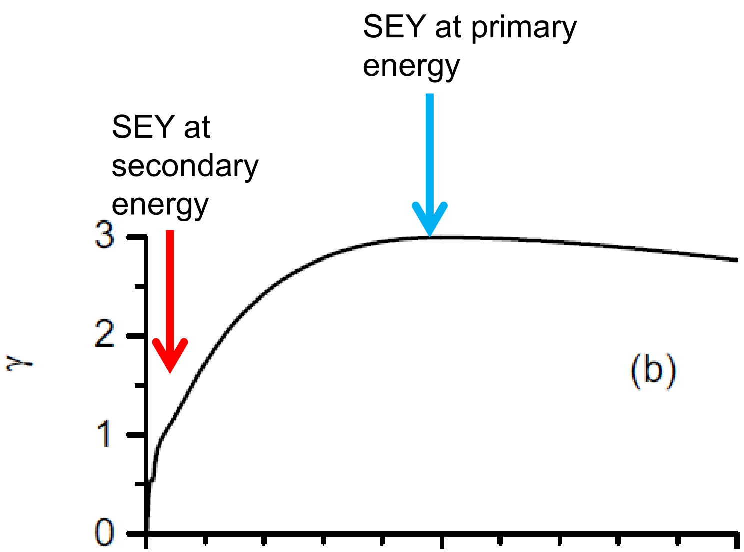

Figure from Sydorenko, PhD thesis (2006) [2]

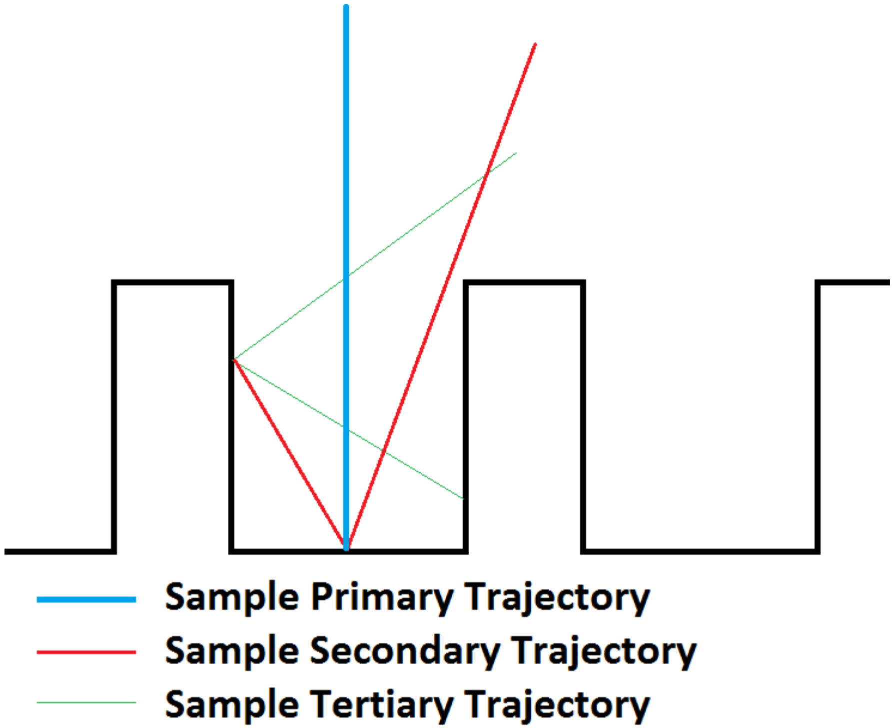

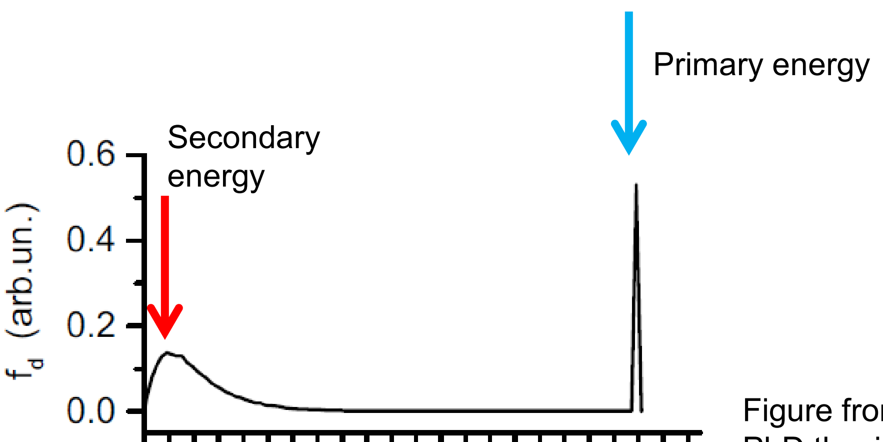

Figure from Sydorenko, PhD thesis (2006) [2]

Primary electrons are of high energy. They emit many secondaries when they hit a surface

Secondary electrons are of low energy. They emit few tertiaries *if* they hit a surface

Candidate geometries

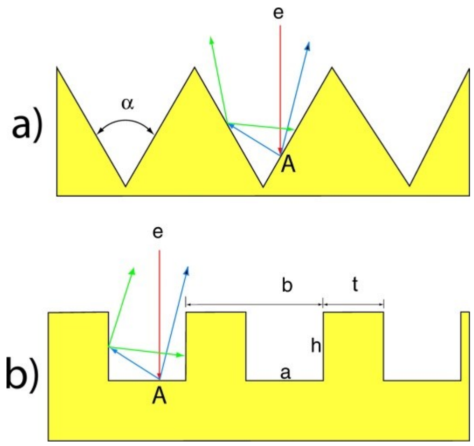

Schematic representation of triangular and rectangular grooves. Figure from Pivi *et. al.*, J. Appl. Phys. (2008) [9]

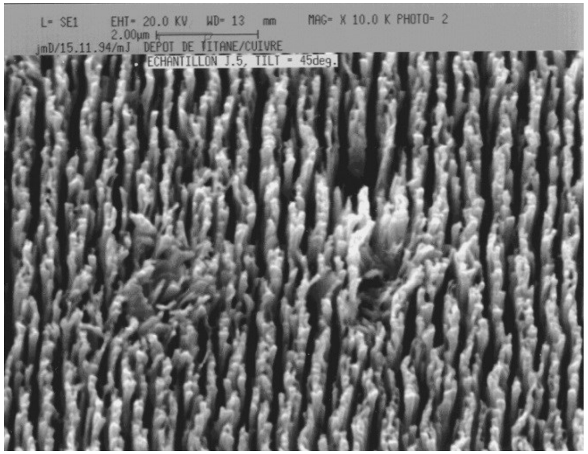

Electron micrograph of “dendritic” copper. Figure from Baglin *et. al.*, Proceedings of EPAC 2000, (2000) [10]

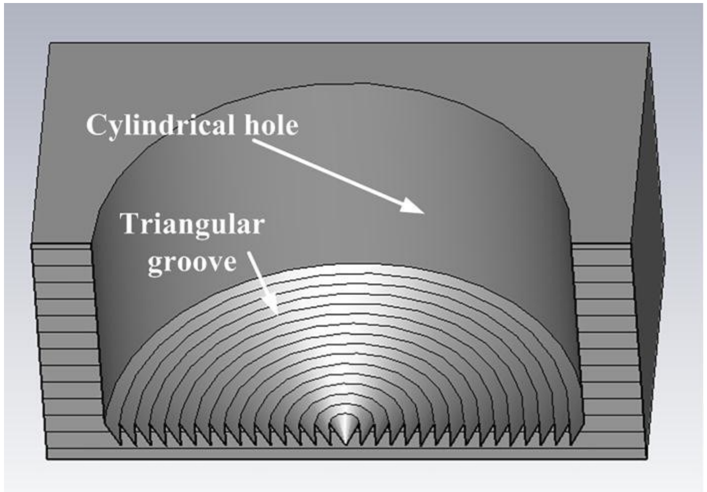

Mix and matching of geometries: Micro-pores floored by triangular grooves. Figure from Ye *et. al.*, J. Appl. Phys. (2017) [11]

Tungsten Fuzz in Tokamak Divertors

Hot tungsten forms fuzz under Helium bombardment. This is expected to occur in ITER's tungsten divertor.

Recent experiments by Patino, Raitses, and Wirz, Appl. Phys. Lett. (2016) measured the SEY from tungsten fuzz and found >60% reduction compared to flat tungsten [19].

SEY in tokamaks may commonly be near unity, Gunn, *Plasma Phys. Control. Fusion* (2012) [20]. This will make ITER's scrape-off layer atypical.

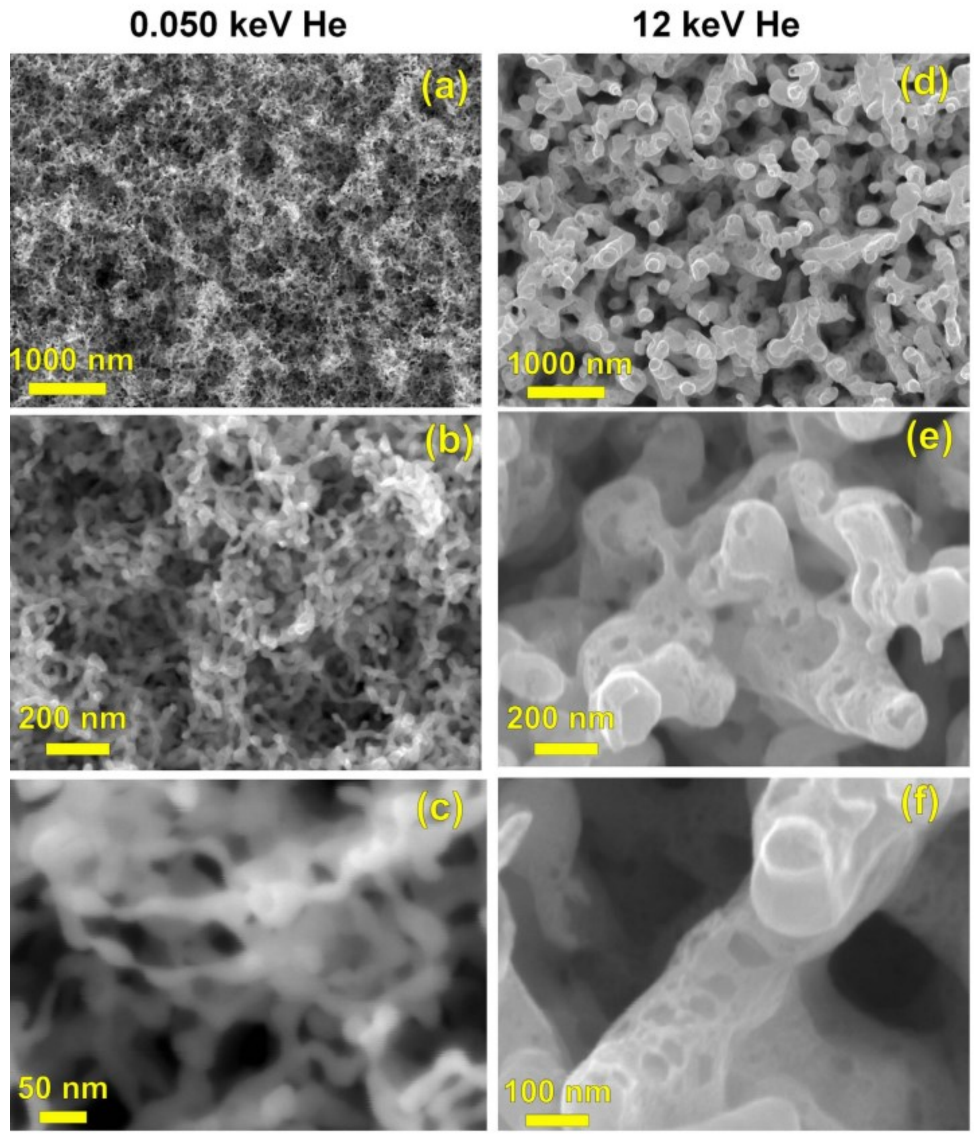

Electron migrographs of tungsten fuzz formed under divertor-like conditions. Wang *et. al.*, *Scientific Reports* (2017) [18]

Other Industrial Applications for these surfaces

Fibrous and fractal-like surfaces are being developed anyway in industry for a variety of applications

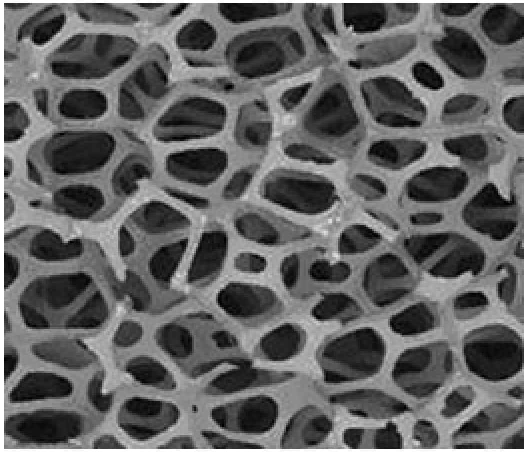

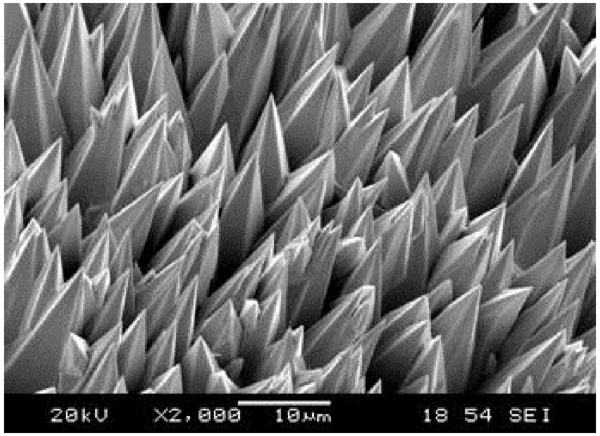

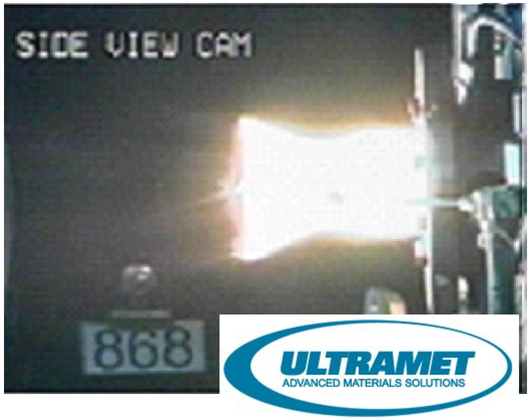

http://www.ultramet.com/

Aerospace companies produce micro- architectured materials for improved thermal resistivity or increased emittance. At right is a radiatively-cooled rocket firing.

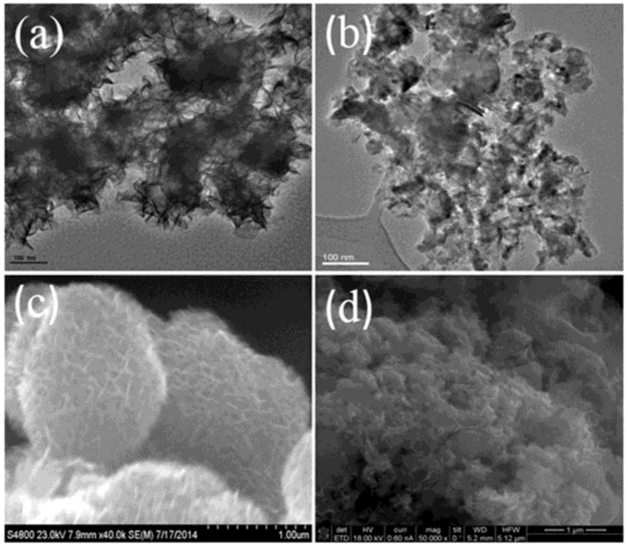

Many chemical catalysts have fractal shapes. Figure from Ramos *et. al.* Scientific Reports (2017) [21]

The tool: Monte-Carlo simulation

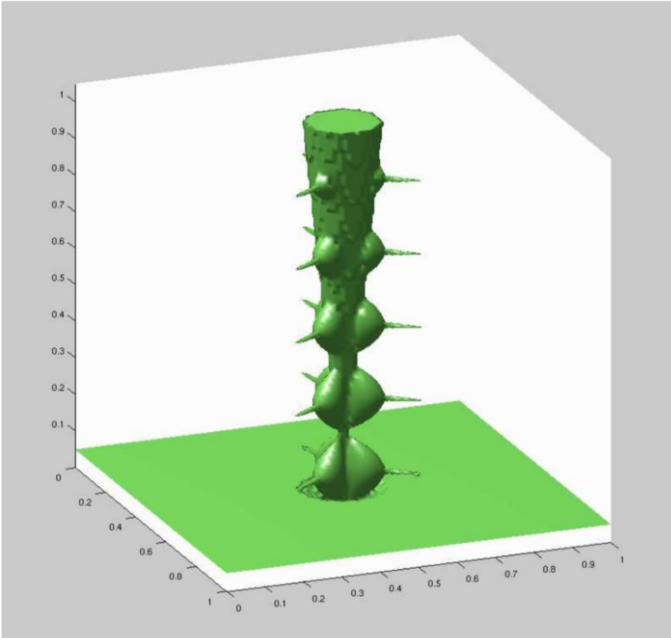

Surfaces implemented as iso-surfaces

Empirical Model at surface:

$$\gamma(E_p,\theta) = \gamma_{max}(\theta) \times \exp\left\{-\left(\frac{\ln\left(\frac{E_p}{E_{max}(\theta)}\right)}{\sqrt{2}\,\sigma}\right)^2\right\}$$

$$\gamma_{max}(\theta) = \gamma_0\left(1 + \frac{k_s\theta^2}{2\pi}\right)$$

$$E_{max}(\theta) = E_0(1 + \frac{k_s\theta^2}{\pi})$$

Graphite: $\gamma_0 = 1.2, E_0 = 325eV, \sigma = 1.6, k_s = 1$

$$f_{el}(E_p) = \exp\left\{1.59 + 3.75\ln(E_p) - 1.37[\ln(E_p)]^2 + 0.12[\ln(E_p)]^3\right\}$$

Adapted from references [1],[12],[13]

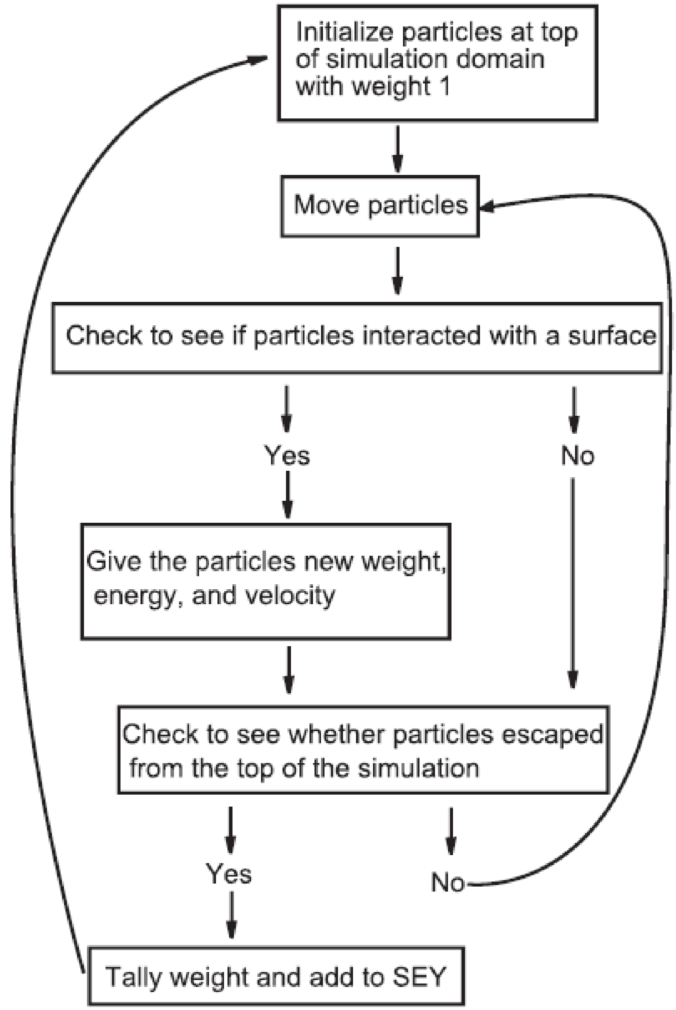

Number of particles: 10^5

Swanson, J. Appl. Phys. (2016) [14]

Our work: Velvet

Swanson and Kaganovich, J. Appl. Phys. (2016) [14]

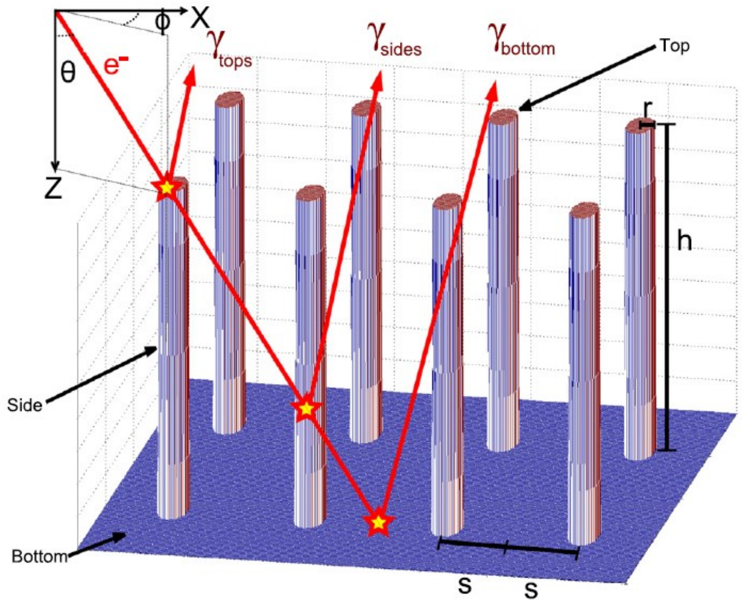

Velvet: regular or irregular lattice of normally-oriented fibers

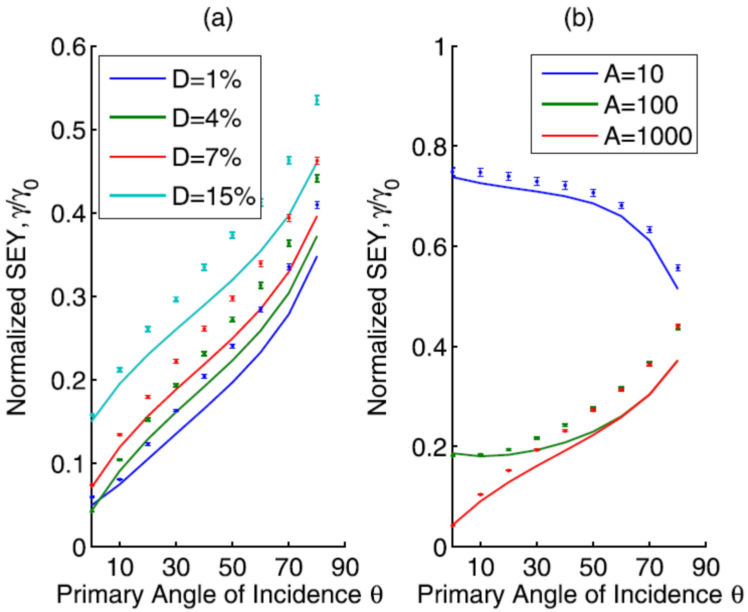

Lines: Analytic model.
Points: Monte-Carlo simulations.

Discrepancy is due to tertiary and higher-order electrons.

Velvet is well-suited to suppressing normally incident primary electrons

Our work: Velvet

Swanson and Kaganovich , J. Appl. Phys. (2016) [14]

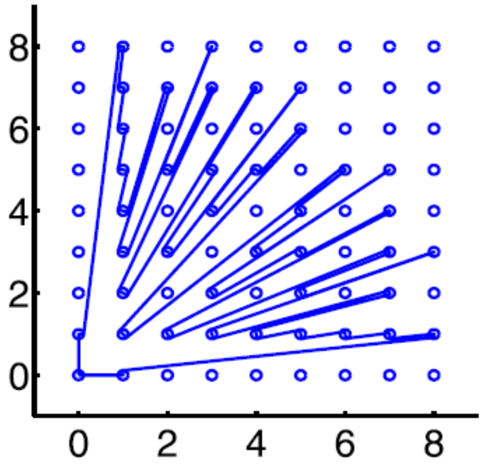

$$u = \frac{\pi}{2} DA = 2rnh$$

u dimensionless parameter, D area packing fraction, A aspect ratio of fibers, r radius of fibers, n area density of fibers, h height of fiber layer

$\mathrm{P}(e)$: Probability of escape into the bulk

$$\gamma_{eff} = \gamma \times \left[\mathrm{P}(e|top)\mathrm{P}(z_{hit} = h) + \mathrm{P}(e|bottom)\mathrm{P}(z_{hit} = 0) + \int dz \mathrm{P}(e|z)\mathrm{P}(z)\right]$$

$$\boxed{1 \times D}$$

$$\boxed{(1-D)e^{-u\tan\theta_1} \times 2\int dt \frac{te^{-ut}}{(1+t^2)^2}}$$

$$\boxed{\frac{2}{\pi}(1-D)\tan\theta_1 \times \int dt \frac{t^2}{(1+t^2)^2} \frac{1-e^{-u(t+\tan\theta_1)}}{t+\tan\theta_1}}$$

(a z integration has already been carried out)
This term dominates in a long, thin velvet
$t = \tan\theta_2$

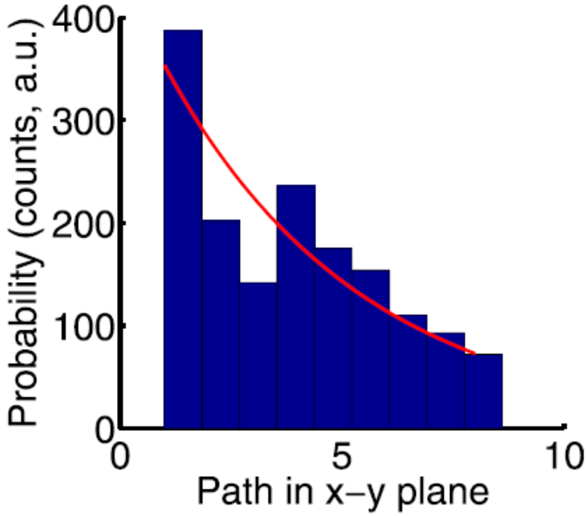

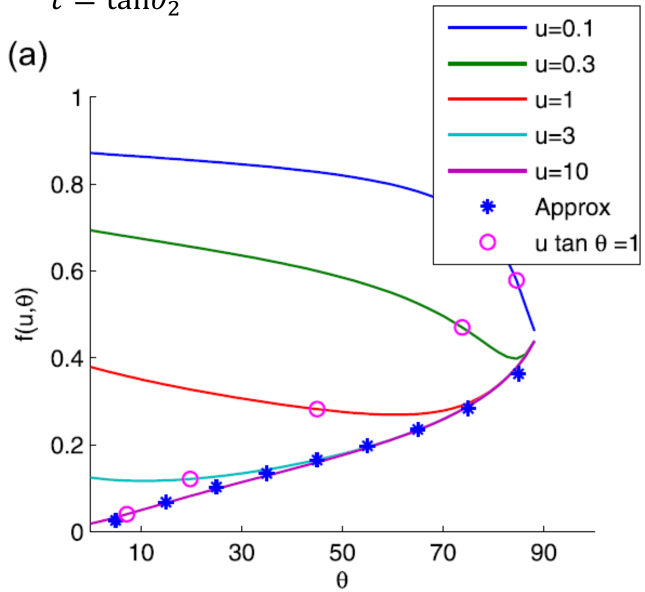

Analytic model approximation:
Probability of whisker intersection is constant per length traveled perpendicular to whisker axis:

$$P(\Delta z) = e^{-u\Delta z\tan\theta_1/h}$$

Recent experiment: Velvet

Jin, Ottaviano, and Raitses , J. Appl. Phys. (2017) [15]

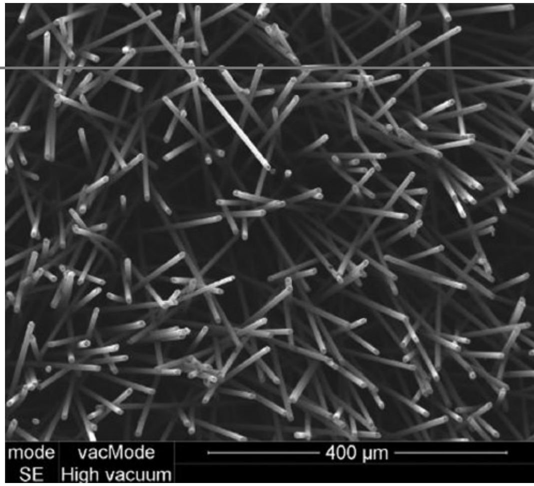

Jin, Ottaviano, and Raitses performed measurements of surfaces with velvet fibers.

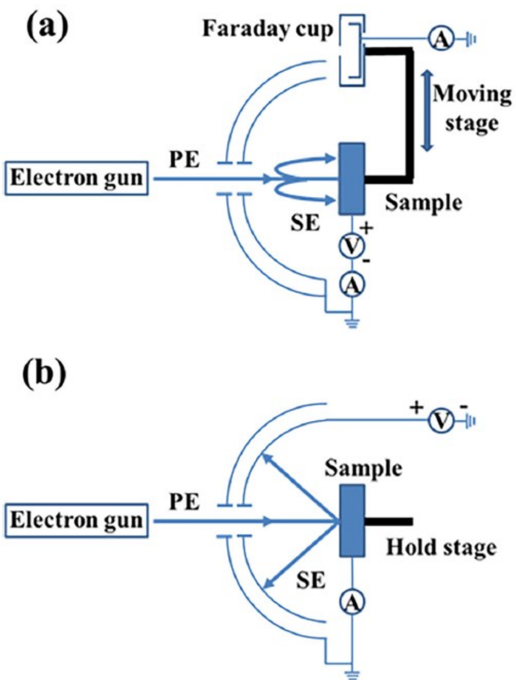

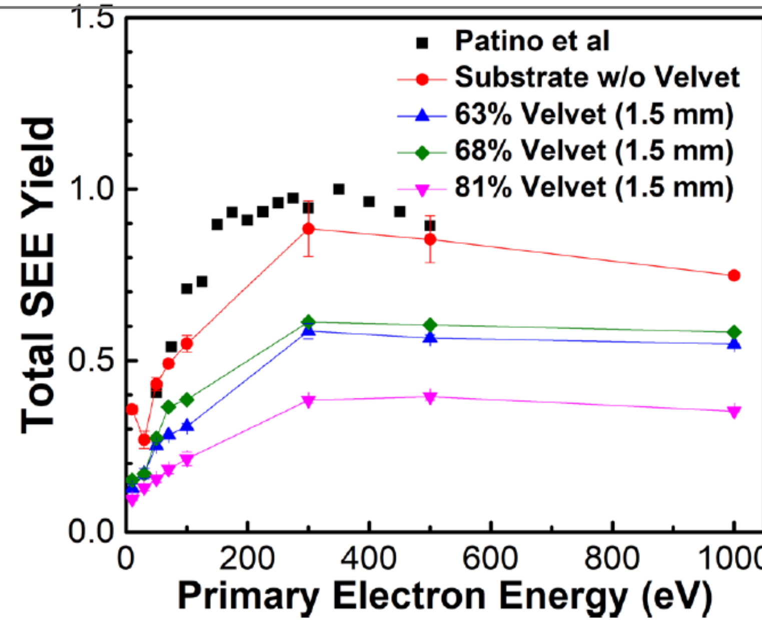

Experimental SEY values for a real carbon velvet. The pink velvet had nominal values: $D = 0.035, A = 430, u = 24$. This measured SEY is a ~65% reduction.

“81%” corresponds to the amount of area as seen from perfectly normal whose view of the substrate is obstructed, a slightly different definition from ours.

Disagreement with experiment could be due to a distribution of axial alignments, rather than the perfectly normal assumed by Swanson & Kaganovich (2016) [14].

Furthermore, our model assumed $\gamma \propto \left(1 + \frac{k_s \theta^2}{2\pi}\right)$, while this paper claims that a $\gamma \propto 1/\cos(\theta)$ relationship is more accurate. Further work is needed to resolve this discrepancy.

Our work: Feathers

Swanson and Kaganovich , J. Appl. Phys. (2017) [16]

Rather than observing, we *designed* a shape that could out-perform other shapes at suppressing SEE. Our shape is two scales of velvet.

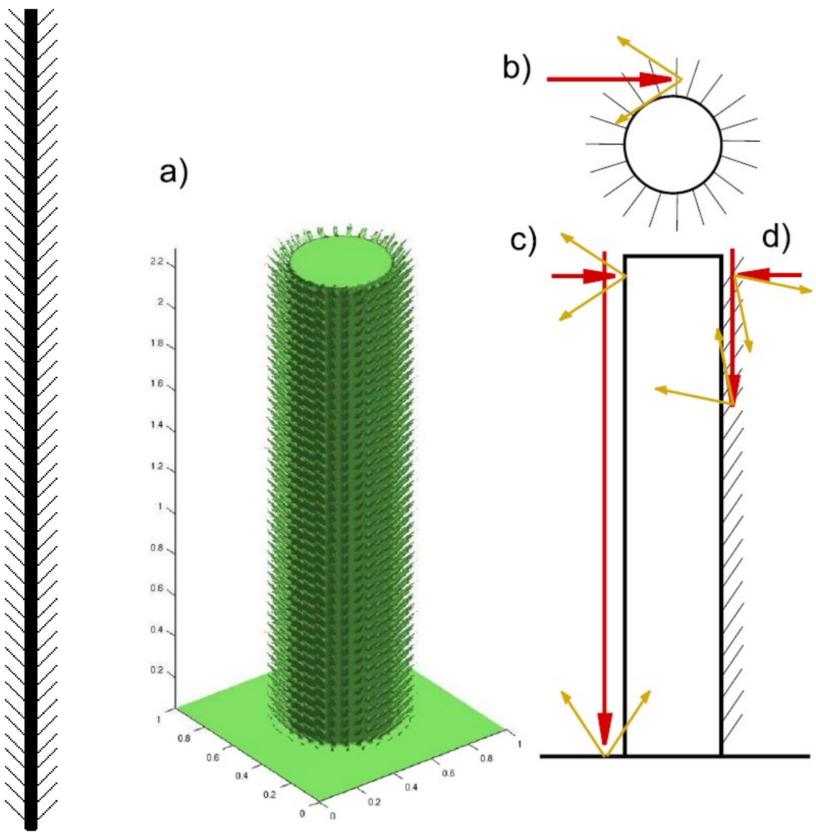

Feather: lattice of normally-oriented fibers *with* smaller, secondary fibers on the sides of *that* fiber.

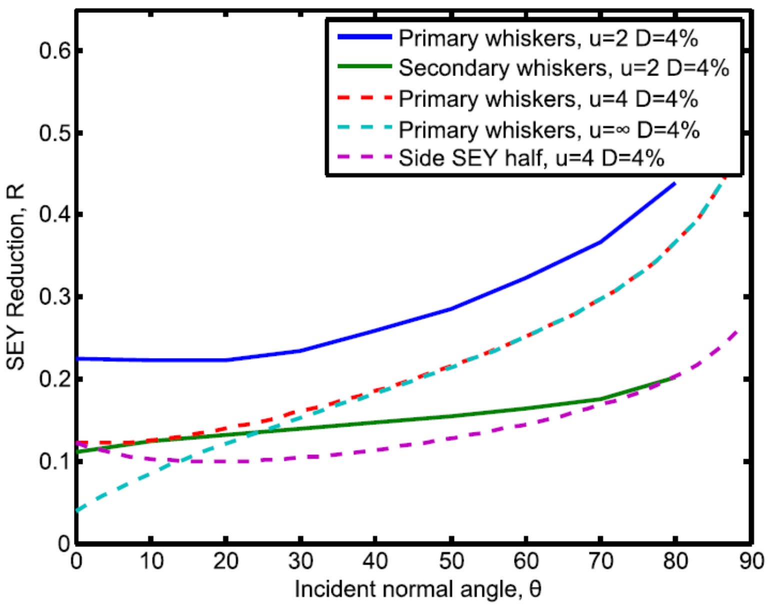

Solid lines: Simulation.
Dashed lines: Numerical Velvet ("primary whisker") result.

"Side SEY half": The SEY from the sides of the whisker is reduced by a factor of 2.

u=4: This SEY trace is that of primary whiskers which are thicker than the primary whisker simulated.

Note that secondary whisker suppress beyond what infinitely long primary whiskers are able to.

Our work: Fuzz/foam

Swanson and Kaganovich , J. Appl. Phys. (2018) [17]

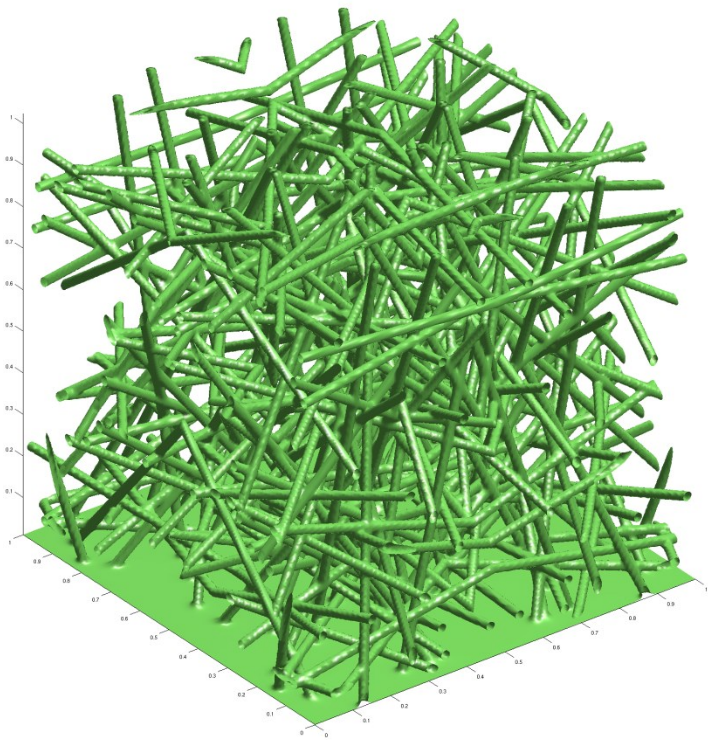

Fuzz/foam: irregular lattice of isotropically-oriented fibers

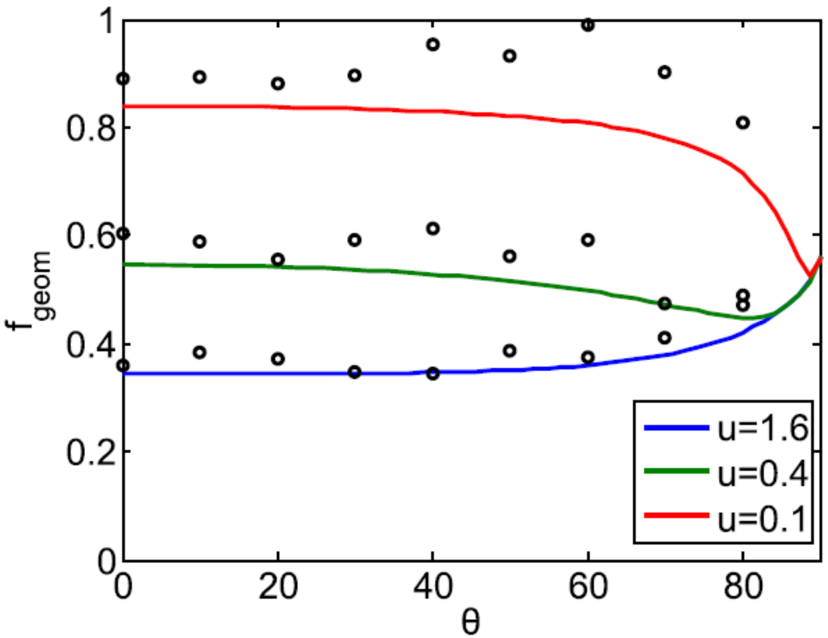

Lines: Analytic model.
Points: Monte-Carlo simulations.
Discrepancy is due to tertiary and higher-order electrons.

Our work: Fuzz/foam

Swanson and Kaganovich , J. Appl. Phys. (2018) [17]

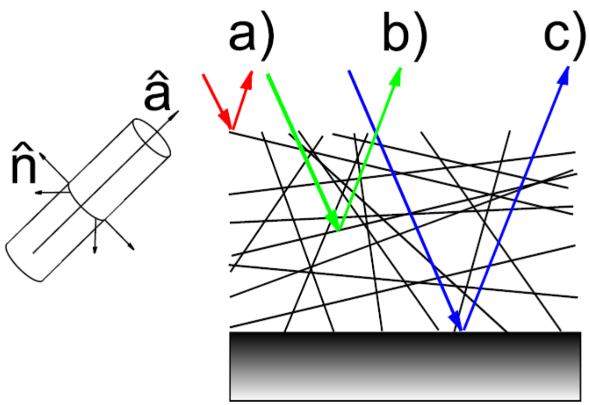

$\bar{u} = DA/2$

The analytic formulae are generalizations of those of velvet to multiple axes of alignment.

In the case of optimal foam (thin fibers, thick fiber layer), SEY can not be reduced to less than 0.3 of its flat value.

$$\gamma_{eff} = \gamma \times \left[D + (1-D)\int_0^1 d\mu_2 2\mu_2 e^{-\left(\frac{1}{\mu}+\frac{1}{\mu_2}\right)\bar{u}} + (1-D)\int_0^1 d\mu_2 \frac{1-e^{-\left(\frac{1}{\mu}+\frac{1}{\mu_2}\right)\bar{u}}}{1+\frac{\mu}{\mu_2}} P(\mu_2|\mu)\right]$$

$$P(\mu_2|\mu) = \frac{4}{\pi}\int_{-1}^{1} dm\,(A_1 \sin\phi_1 + B_1\phi_1)\,(A_2 \sin\phi_2 + B_2\phi_2)$$

$$A_{1,2} = \sqrt{(1-m^2)(1-\mu_{1,2}^2)}, B_{1,2} = m\mu_{1,2}$$

$$\mu = \cos\theta$$

Analytic model approximation: Probability of whisker intersection is constant per length traveled perpendicular to whisker axis; field of whiskers is infinite sum of infinitesimal fields of uniformly aligned whiskers:

$$P(\Delta z) = e^{\frac{\bar{u}\Delta z}{h\cos\theta_1}}$$

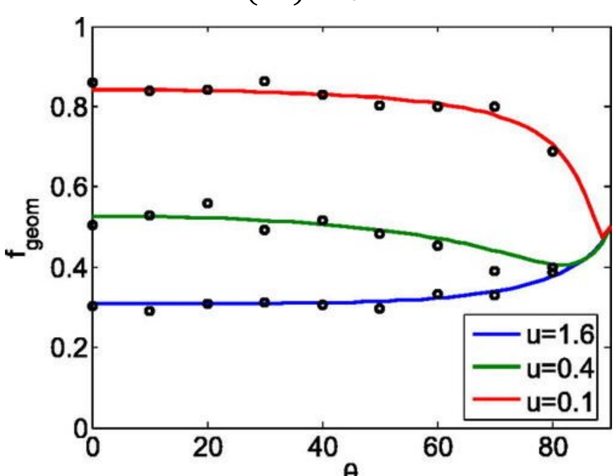

If no teritary electrons are considered, the model is accurate.

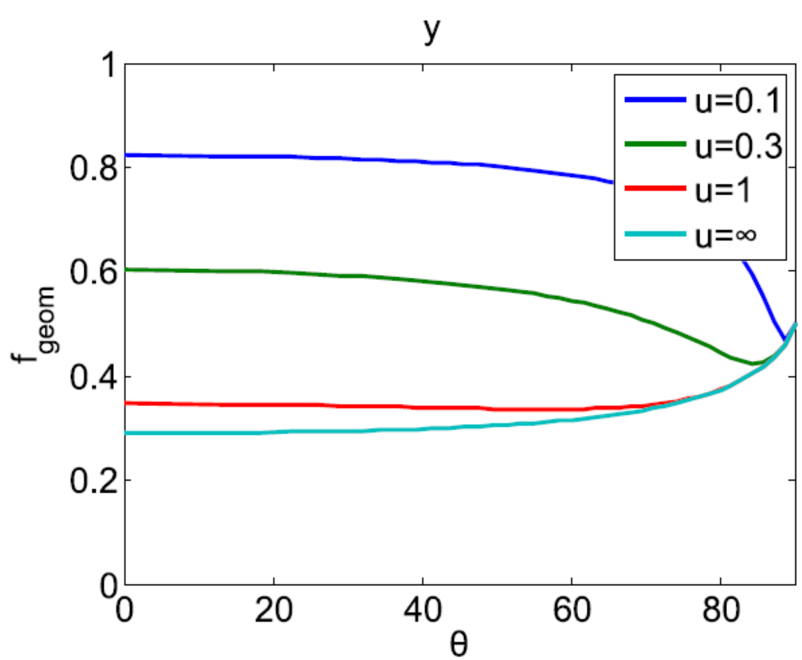

Conclusions

- Control over secondary electron emission has theoretical and practical implications

- In recent years, an avenue for such control has been complex surface geometry

- Such surface geometries can be evaluated by Monte-Carlo simulations before being experimentally measured

- Fibrous surfaces, which are developed for other purposes, are well-suited to secondary electron suppression

Bibliography

[1] J. Scholtz et al., “Secondary electron emission properties,” Philips J. Res. 50, 375 (1996).
[2] Sydorenko, Dmytro. “Particle-in-Cell Simulations of Electron Dynamics in Low Pressure Discharges with Magnetic Fields,” 2006. https://ecommons.usask.ca/handle/10388/etd-06142006-111353.
[3] Vtorichnaya Elektronnaya Emissiya, edited by I. M. Bronstein and B. S. Fraiman (Nauka, Movkva, 1969), p. 340 (in Russian).
[4] Campanell, M. D., A. V. Khrabrov, and I. D. Kaganovich. “Absence of Debye Sheaths Due to Secondary Electron Emission.” *Physical Review Letters* 108, no. 25 (June 18, 2012): 255001.
[5] Kushner, M. J. “Mechanisms for Power Deposition in Ar/SiH4 Capacitively Coupled RF Discharges.” *IEEE Transactions on Plasma Science* 14, no. 2 (April 1986): 188–96. https://doi.org/10.1109/TPS.1986.4316522.
[6] J. R. M. Vaughan, “Multipactor,” IEEE Trans. Electron Devices 35, 1172–1180 (1988).
[7] I. Kaganovich, Y. Raitses, D. Sydorenko, and A. Smolyakov, “Kinetic effects in a Hall thruster discharge,” Phys. Plasmas, vol. 14, no. 5, p. 057104, May 2007.
[8] Zimmermann, Frank. “A Simulation Study of Electron Cloud Instability and Beam Induced Multipacting in the LHC,” 1997.
[9] M. T. F. Pivi et al., “Sharp reduction of the secondary electron emission yield from grooved surfaces,” J. Appl. Phys. 104, 104904 (2008).
[10] V. Baglin, J. Bojko, O. Grabner, B. Henrist, N. Hilleret, C. Scheuerlein, and M. Taborelli, “The secondary electron yield of technical materials and its variation with surface treatments,” in Proceedings of EPAC 2000, 26–30 June 2000, Austria Center, Vienna, pp. 217–221.
[11] M. Ye, W. Dan, and H. Yongning, “Mechanism of total electron emission yield reduction using a micro-porous surface,” J. Appl. Phys. 121(12), 124901 (2017).
[12] J. Vaughan, “A new formula for secondary emission yield,” IEEE Trans. Electron Devices 36, 1963 (1989).
[13] M. Patino, Y. Raitses, B. Koel, and R. Wirz, “Application of Auger spectroscopy for measurement of secondary electron emission from conducting material for electric propulsion devices,” in 33rd International Electric Propulsion Conference (IPEC), The George Washington University, Washington, DC, USA, 6–10 October 2013.
[14] Swanson, Charles, and Igor D. Kaganovich. “Modeling of Reduced Effective Secondary Electron Emission Yield from a Velvet Surface.” Journal of Applied Physics 120, no. 21 (December 7, 2016): 213302. https://doi.org/10.1063/1.4971337.
[15] Jin, Chenggang, Angelica Ottaviano, and Yevgeny Raitses. “Secondary Electron Emission Yield from High Aspect Ratio Carbon Velvet Surfaces.” *Journal of Applied Physics* 122, no. 17 (November 1, 2017): 173301. https://doi.org/10.1063/1.4993979.
[16] Swanson, Charles, and Igor D. Kaganovich. “‘Feathered’ Fractal Surfaces to Minimize Secondary Electron Emission for a Wide Range of Incident Angles.” Journal of Applied Physics 122, no. 4 (July 24, 2017): 043301. https://doi.org/10.1063/1.4995535
[17] Swanson, Charles, and Igor D. Kaganovich. “Modeling of Reduced Secondary Electron Emission Yield from a Foam or Fuzz Surface.” *Journal of Applied Physics* 123, no. 2 (January 10, 2018): 023302. https://doi.org/10.1063/1.5008261.
[18] Wang, Kun, R. P. Doerner, M. J. Baldwin, F. W. Meyer, M. E. Bannister, Amith Darbal, Robert Stroud, and Chad M. Parish. “Morphologies of Tungsten Nanotendrils Grown under Helium Exposure.” *Scientific Reports* 7 (February 14, 2017): 42315. https://doi.org/10.1038/srep42315.
[19] M. Patino , Y. Raitses , and R. Wirz , “ Secondary electron emission from plasma-generated nanostructured tungsten fuzz,” Appl. Phys. Lett. **109**(20), 201602 (2016). https://doi.org/10.1063/1.4967830
[20] Gunn J P 2012 *Plasma Phys. Control. Fusion* **54** 085007
[21] Ramos, Manuel, Félix Galindo-Hernández, Ilke Arslan, Toby Sanders, and José Manuel Domínguez. “Electron Tomography and Fractal Aspects of MoS 2 and MoS 2 /Co Spheres.” *Scientific Reports* 7, no. 1 (September 26, 2017): 12322. https://doi.org/10.1038/s41598-017-12029-8.